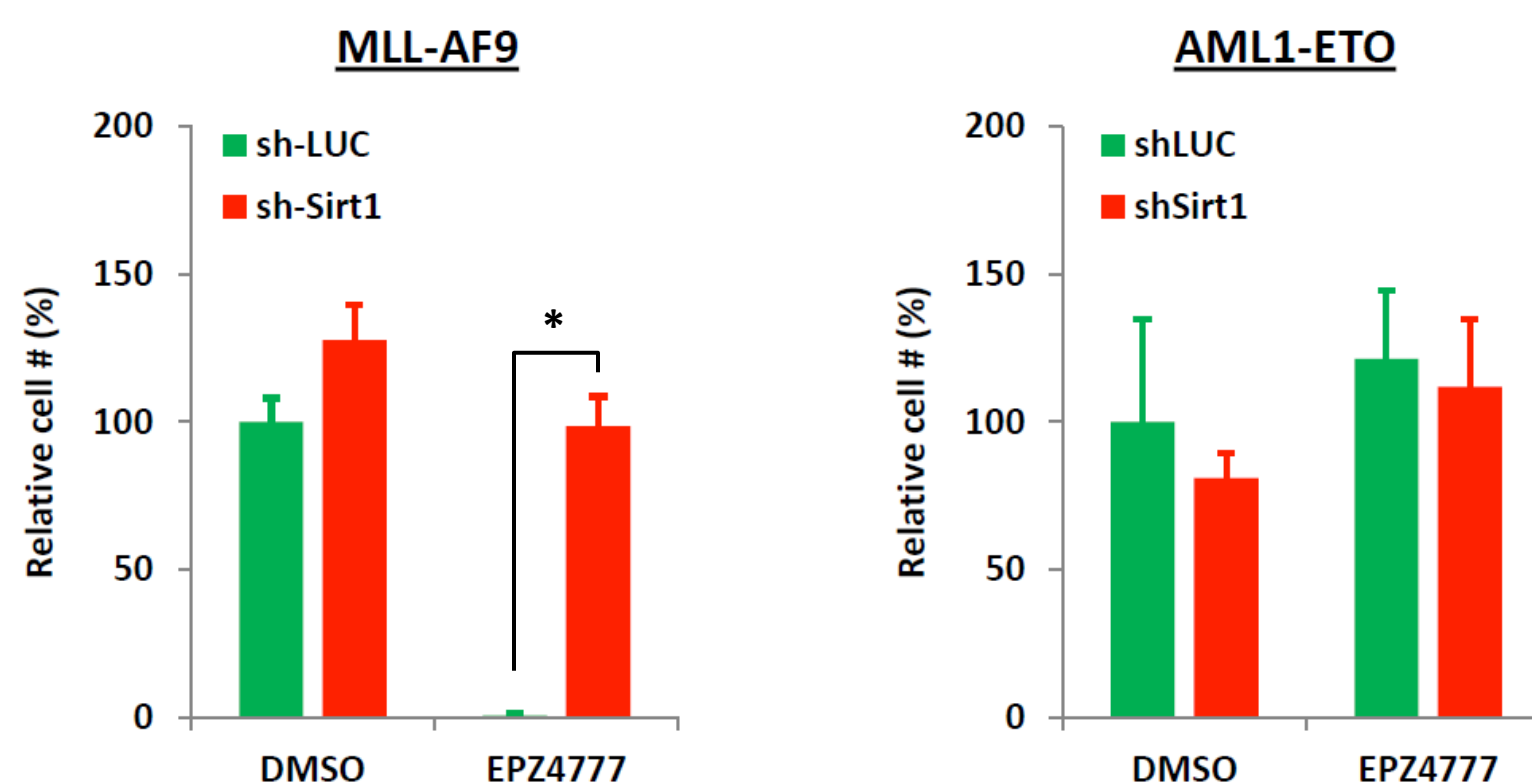


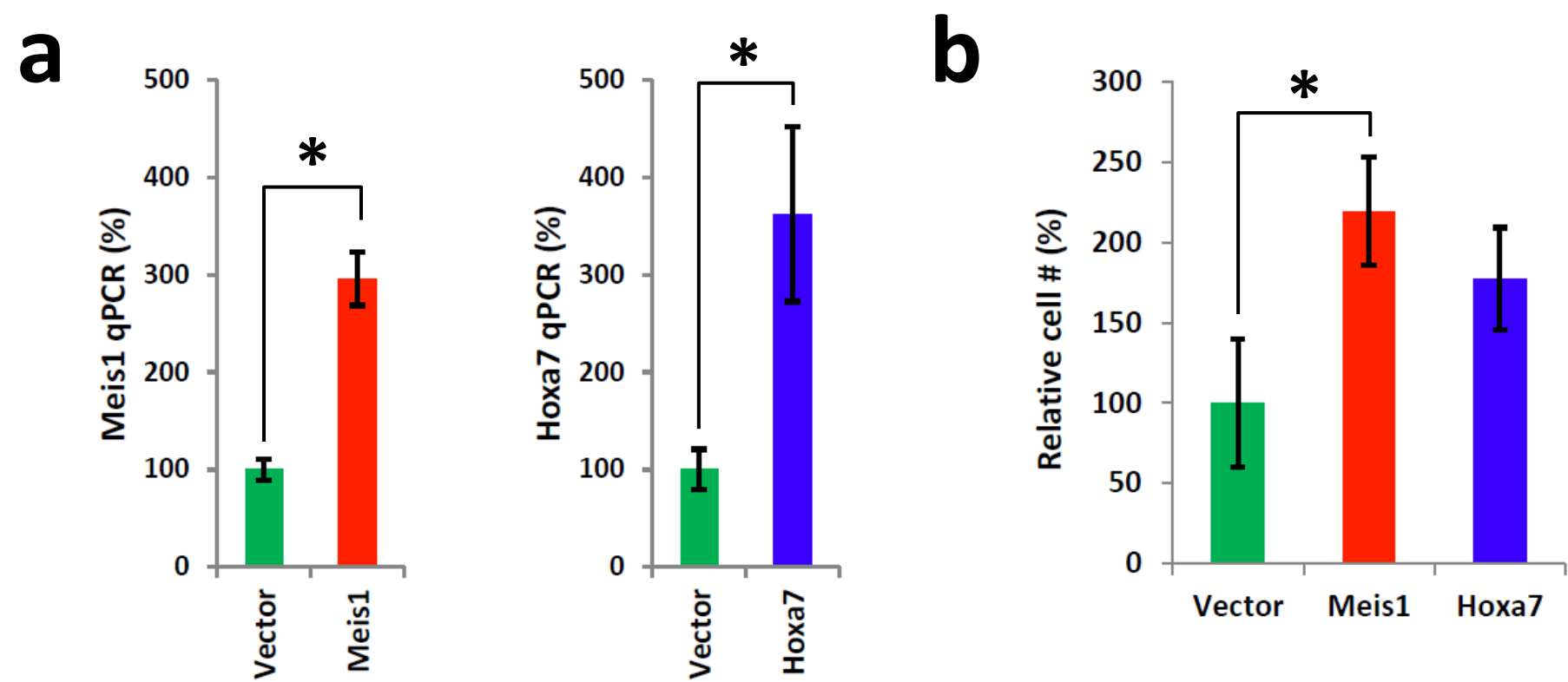
Suppl. Figure 1. Screen validation for top “candidate antagonists of *Dot1L*”

(a) Number of genes with one (gray), two (cyan) or three (red) shRNA scored in the enriched 934 shRNA pool from the genome-scale RNAi screen using the *Dot1L*-deletion model. Numbers in parentheses indicate the expected number of genes for each category based on an average of 5 shRNA per gene in the genome-scale library. Genes with three shRNA scored in the screen are *Sirt1*, *Hmg20b* and *Gm4763*. Genes with more than 8 shRNA in the library were excluded from the analysis. (b) Effect of EPZ4777 on the proliferation of murine *MLL-AF9* leukemic cells transduced with the indicated shRNA constructs. Cells were cultured in the presence of DMSO (open) or EPZ4777 (solid) for 9 days. (c) Frequency of the indicated sh-*Sirt1* in the genome-scale RNAi screen. (d) RT-qPCR of *Sirt1* in *MLL-AF9* leukemic cells transduced with indicated sh-*Sirt1* or sh-*LUC* constructs. Data represent mean \pm s.d. of a triplicated experiment. * $P < 0.05$ to sh-*LUC*.



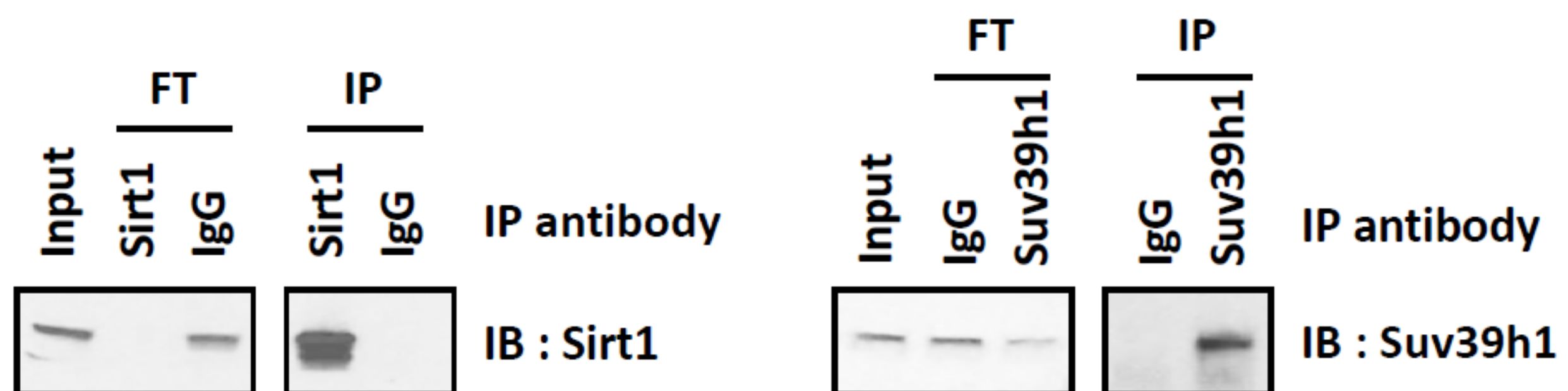
Suppl. Figure 2. Effect of *Sirt1* knockdown and *Dot1L* inhibition on *MLL-AF9* and *AML1-ETO* murine leukemic cells.

Effect of *Sirt1* knockdown on the proliferation of *MLL-AF9* (left) and *AML1-ETO* (right) leukemic cells treated with DMSO or EPZ4777 (3 μ M) for 9 days. Cells were derived from retroviral-mediated transduction of *MLL-AF9* or *AML1-ETO* fusion protein into mouse Lin⁻Sca1⁺cKit⁺ bone marrow hematopoietic progenitors. Data represent mean \pm s.d. of a triplicated experiment. * $P < 0.01$.



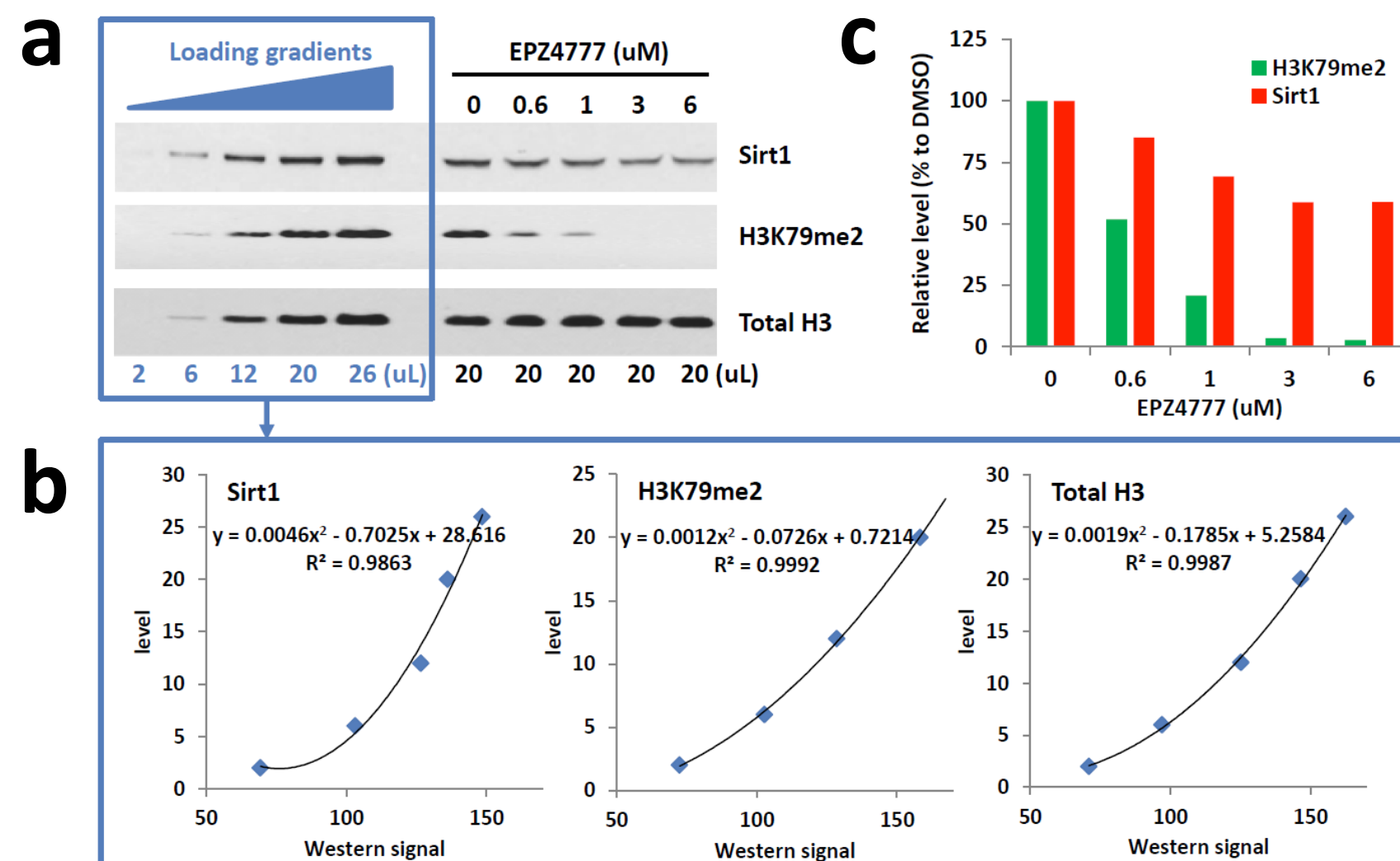
Suppl. Figure 3. Retroviral-mediated overexpression of *Meis1* or *Hoxa7* increases the cell number in *MLL-AF9* cell cultures.

(a) RT-qPCR of *Meis1* (left) and *Hoxa7* (right) in *MLL-AF9* leukemic cells transduced with MSCV-puro viruses expressing *Meis1* (red), *Hoxa7* (blue), and vector control (green). Data represent mean \pm s.d. of a duplicated experiment. * $P < 0.05$. (b) Effect of *Meis1* or *Hoxa7* overexpression on the cell number of *MLL-AF9* leukemic cells cultured for 9 days. Data represent mean \pm s.d. of a triplicated experiment. * $P < 0.05$.



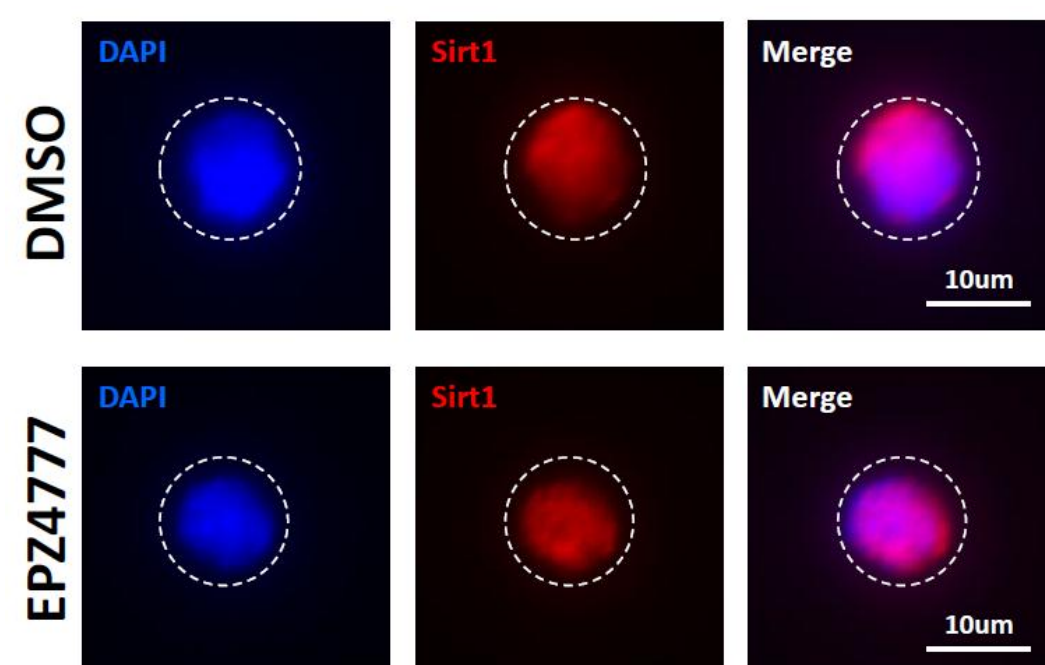
Suppl. Figure 4. Validation of Sirt1 and Suv39h1 antibodies for immunoprecipitation.

Lysate of murine *MLL-AF9* leukemia cells was incubated with 10 μ g/ml of anti-Sirt1 (Abcam; Ab12193; left panel), anti-Suv39h1 (Cell signaling; cat#8729; right panel) or normal IgG antibody overnight, and captured by protein A/G beads (Millipore) for 2 hours. The input, flow through (FT) and immunoprecipitated (IP) samples were then immunoblotted for Sirt1 (left panel) and Suv39h1 (right panel).



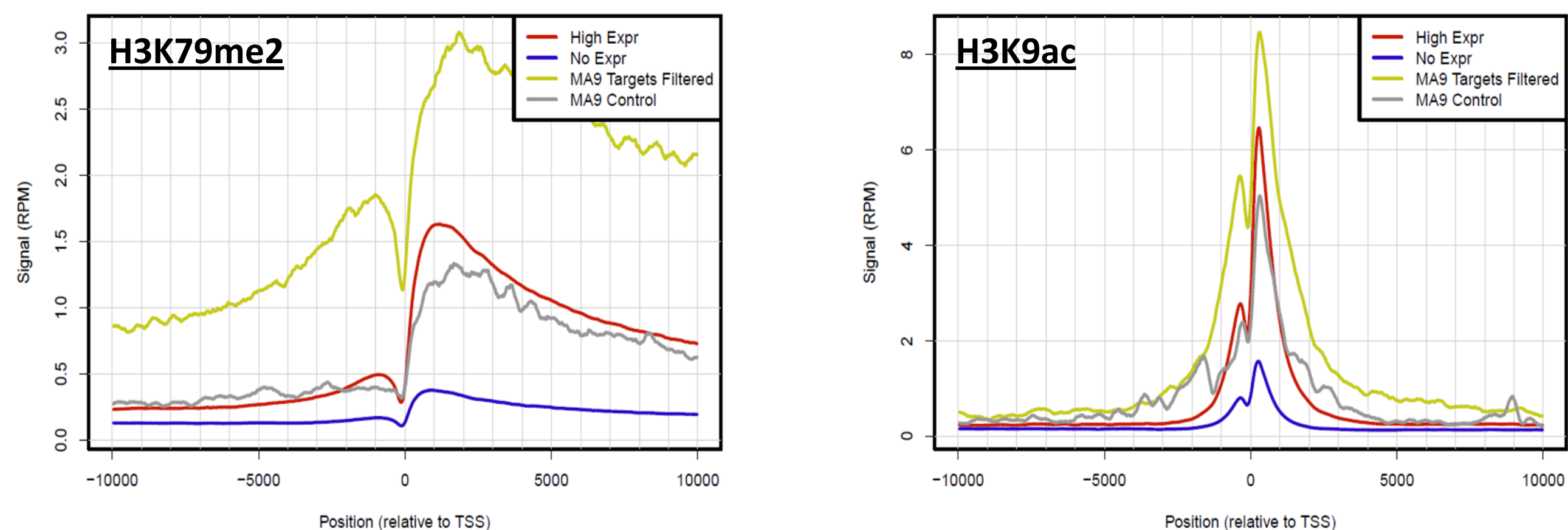
Suppl. Figure 5. Effect of Dot1L inhibition on Sirt1 and H3K79me2 levels in *MLL-AF9* leukemic cells.

(a) Semi-quantitative immunoblot analysis for Sirt1 (Abcam; Ab12193), H3K79me2 (Abcam; Ab3594) and total histone H3 (Abcam; Ab3594) levels in *MLL-AF9* leukemic cells for (left) loading gradients (2 – 26 uL) of lysate from untreated cells, and (right) lysates (20 uL each) from cells treated with various concentrations of DOT1L inhibitor EPZ4777 (0 – 6 uM). (b) Standard curves of Sirt1, H3K79me2 and total histone H3 derived from the loading gradients and densitometry analysis using ImageJ Software. (c) Relative levels of Sirt1 and H3K79me2 in *MLL-AF9* leukemic cells treated with various concentrations of EPZ4777 were measured by densitometry (ImageJ software) and standard curve fitting. Sirt1 and H3K79me2 levels were normalized to the total histone H3 level of each sample. A nearly complete loss of H3K79me2, and a mild reduction (about 30% less) of Sirt1 protein, was observed in cells treated with more than 3 uM EPZ4777 as compared to the DMSO control condition.



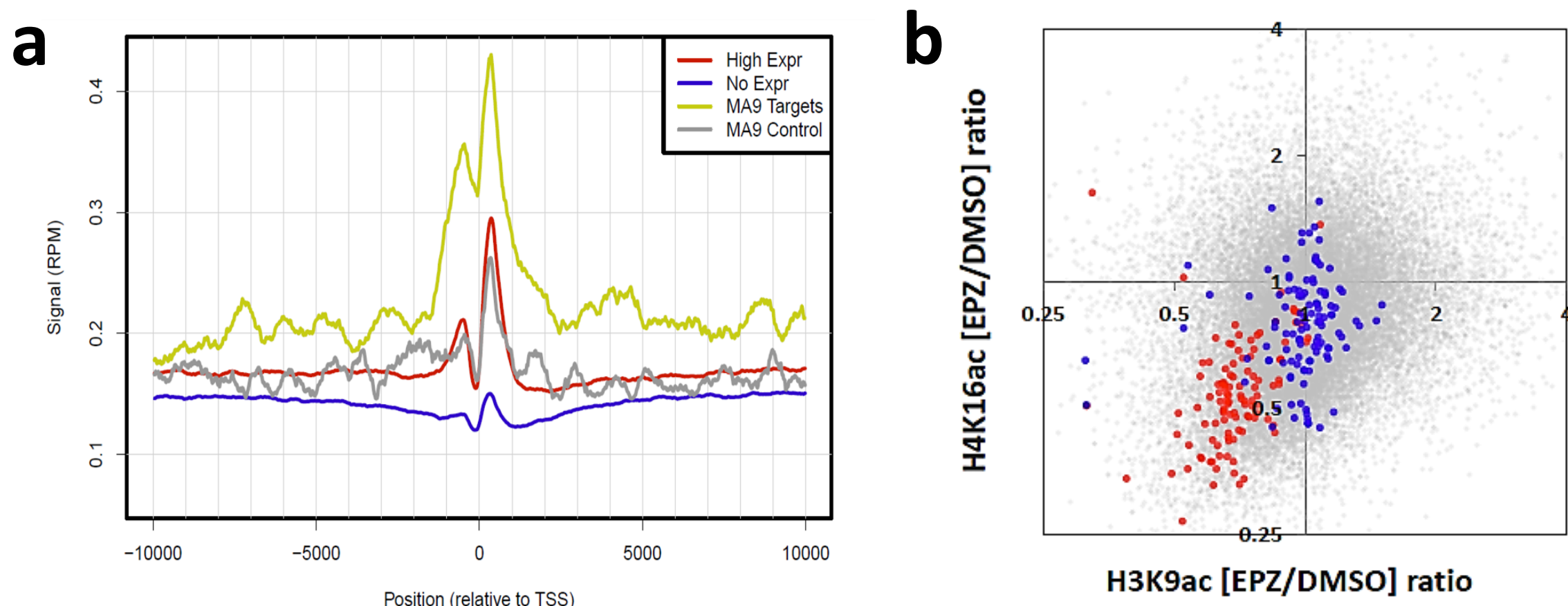
Suppl. Figure 6. Dot1L inhibition does not alter the subcellular distribution of Sirt1 protein in *MLL-AF9* leukemic cells.

Immunofluorescence of *MLL-AF9* leukemic cells cultured in DMSO versus EPZ4777 (3 uM). Cells were stained with DAPI (blue; nucleus) and Sirt1 (red; Ab12193 from Abcam). The white-dashed circles indicate the shape of the cells. DOT1L inhibitor treatment does not induce noticeable changes in the subcellular distribution of Sirt1 protein, which remains predominantly localized in the nucleus (overlaps with DAPI stain) of *MLL-AF9* leukemic cells.



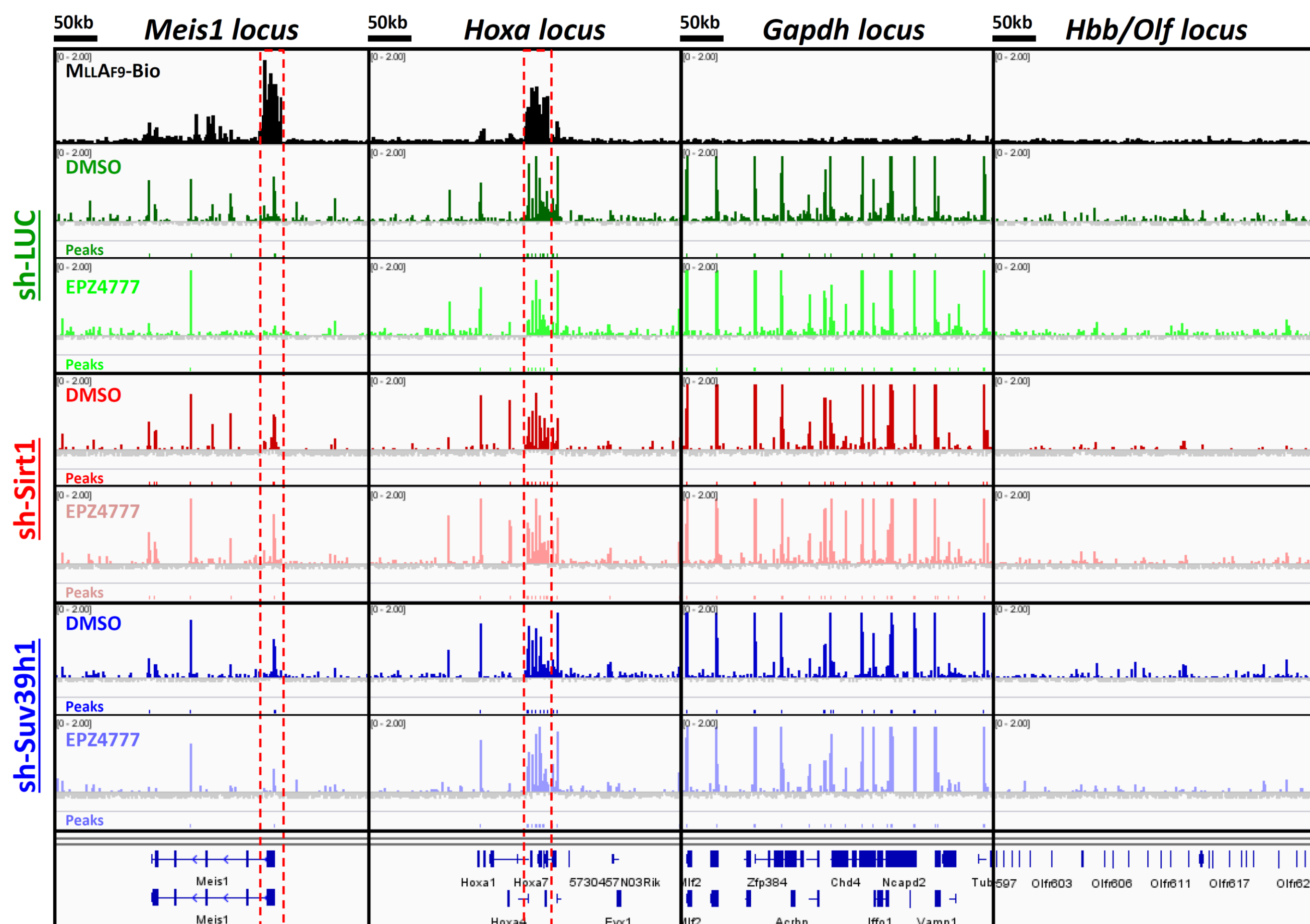
Suppl. Figure 7. Meta analysis of ChIP-seq data from murine *MLL-AF9* leukemia.

Level (y-axis; reads per million) and position (x-axis; ± 10 kb centered to TSS) of H3K79me2 and H3K9ac at highly expressed (red), not expressed (blue), *MLL-AF9* bound target (yellow) and *MLL-AF9* non-target control (gray; from [Bernt et al. 2011 Cancer Cell](#)) genes.



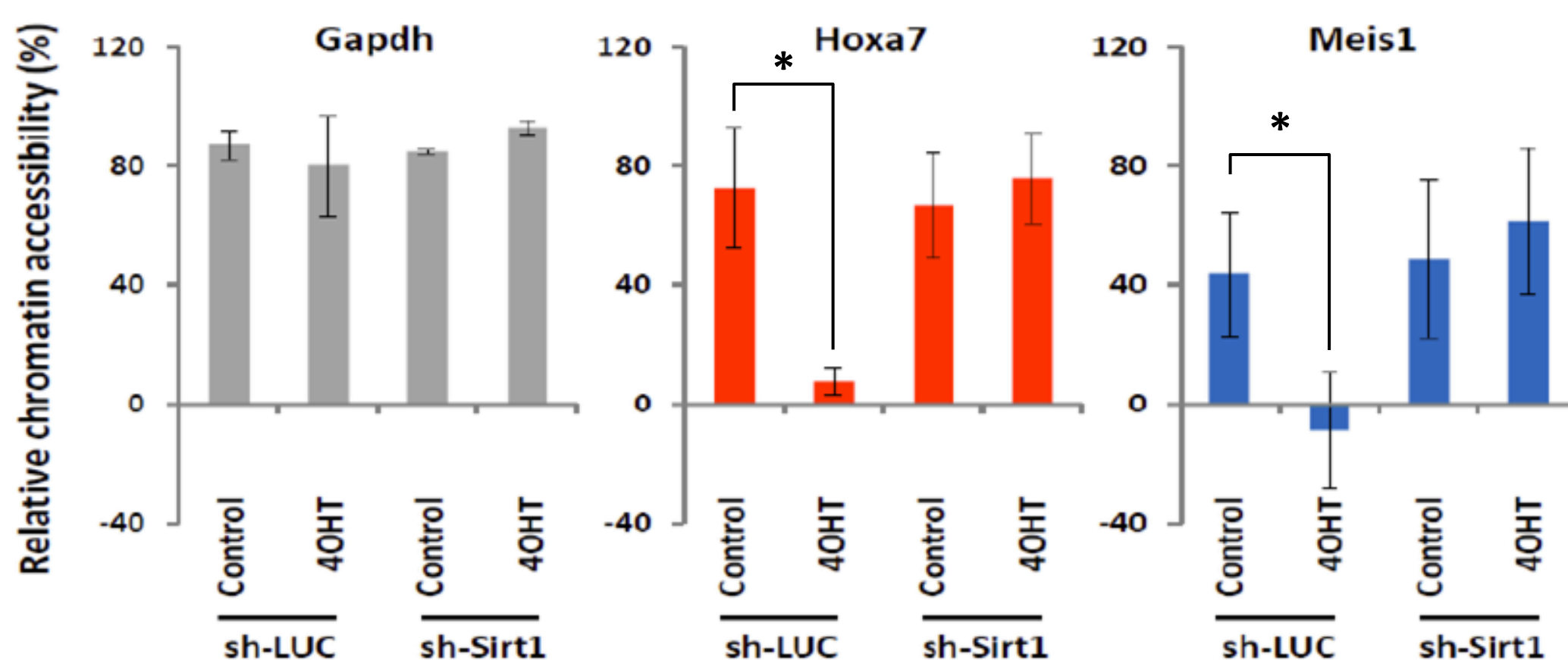
Suppl. Figure 8. ChIP-seq analysis of H4K16ac in murine *MLL-AF9* leukemia.

(a) Meta analysis showing level (y-axis; reads per million) and position (x-axis; ± 10 kb centered to TSS) of H4K16ac at highly expressed (red), not expressed (blue), *MLL-AF9* bound target (yellow) and *MLL-AF9* non-target control (gray; from [Bernt et al. 2011 Cancer Cell](#)) genes. (b) Scatterplots showing changes in H3K9ac level (x-axis; Abcam ab4441) in correlation to changes in H4K16ac level (y-axis; Millipore 17-10101) at TSS ± 2 kb regions in *MLL-AF9* leukemic cells cultured in EPZ4777 (3 uM) versus DMSO for 6 days. Gray dots represent all genes in the genome, and the *MLL-AF9* targets in sh-*LUC* (red dots) or sh-*Sirt1* (blue dots) transduced cells are highlighted.



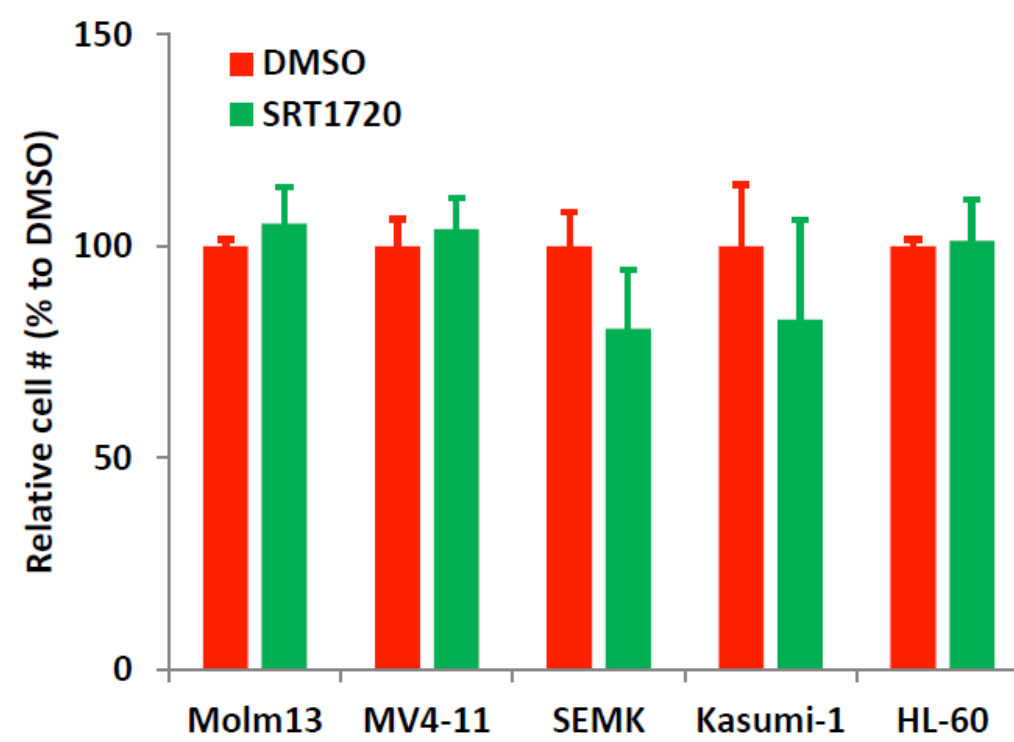
Suppl. Figure 9. ATAC-seq chromatin accessibility profiles.

Screen shots showing ATAC-seq profiles at MLL-AF9 bound target (*Hoxa* cluster and *Meis1*), active gene (*Gapdh*) and silent gene (*Hbb/Olf*) loci in sh-LUC (clone D11; green), sh-Sirt1 (clone A1; red) and sh-Suv39h1 (clone C2; blue) transduced *MLL-AF9* leukemic cells cultured in DMSO or 1 μ M EPZ4777 for 6 days. The core occupied regions for MLL-AF9 are highlighted (red-dashed boxes), and the accessible chromatin regions based on ATAC-seq signal are indicated (Peaks).



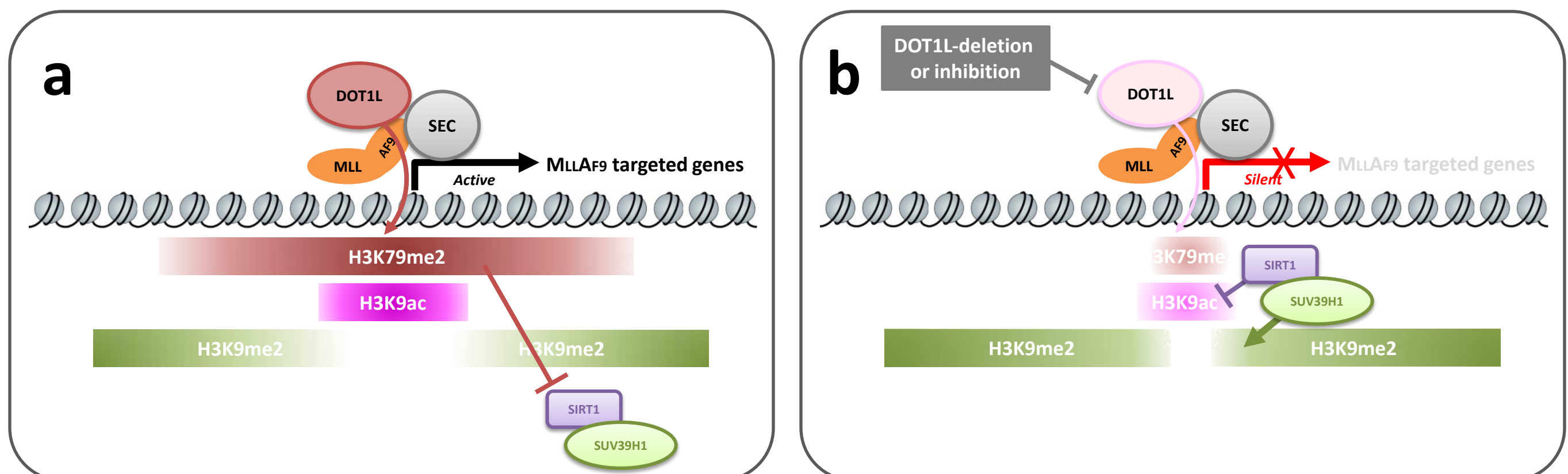
Suppl. Figure 10. Knockdown of *Sirt1* maintains chromatin accessibility at *Hoxa7* and *Meis1* upon deletion of *Dot1l*.

To validate our ATAC-seq transposase accessibility assay (shown in Fig. 5i), we used nuclease digestion of chromatin and qPCR to detect chromatin accessibility at *Hoxa7* and *Meis1* loci in sh-LUC (clone D11) or sh-Sirt1 (clone A1) transduced *MLL-AF9-Dot1l^{fl/fl}-CreER* leukemic cells under control and *Dot1l*-excised (4OHT) conditions. Samples were processed and analyzed using EpiQ Chromatin Analysis Kit according to the manufacturer's protocol (Bio-Rad). The *Gapdh* locus served as a positive control gene for accessible chromatin. Data represent mean \pm s.d. of two experiments. * $P < 0.05$.



Suppl. Figure 11. SRT1720 treatment alone induces limited effect on the cell number of human leukemic cell cultures.

Effect of SRT1720 (1 μ M) on the proliferation of human *MLL*-rearranged Molm13 (*MLL-AF9*), MV4-11 (*MLL-AF4*) and SEMK2 (*MLL-AF4*); and non-*MLL*-rearranged Kasumi-1 (*AML-ETO*) and HL-60 leukemic cell lines cultured for 17 days. Data represent mean \pm s.d. of a duplicated experiment.



Suppl. Figure 13. Model of Regulation of MLL-AF9 Target Genes by DOT1L, SIRT1 and SUV39H1 in *MLL-AF9* leukemia.

(a) Proposed model for MLL-AF9/DOT1L-driven gene expression in *MLL-AF9* leukemia. SEC: super elongation complex.
 (b) Involvement of SIRT1/SUV39H1-mediated repressive mechanisms in silencing MLL-AF9 target gene expression after suppression of DOT1L.